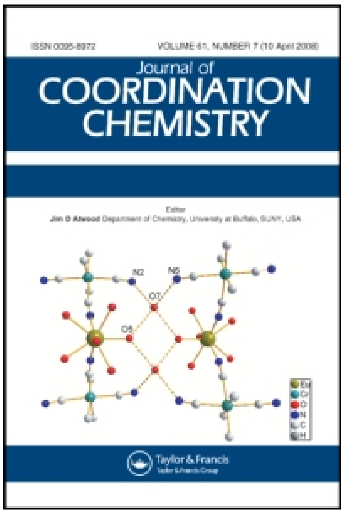

Journal of Coordination Chemistry
Publication details, including instructions for authors and subscription information:
http://www.informaworld.com/smpp/title~content=t713455674

Metal-organic supramolecular architectures derived from a new zwitterionic dicarboxylate ligand

Xiu-Mei Zhang[a]; Xiu-Bing Li[a]; En-Qing Gao[a]
[a] Shanghai Key Laboratory of Green Chemistry and Chemical Processes, Department of Chemistry, East China Normal University, Shanghai 200062, P.R. China

First published on: 13 December 2010

To cite this Article Zhang, Xiu-Mei , Li, Xiu-Bing and Gao, En-Qing(2011) 'Metal-organic supramolecular architectures derived from a new zwitterionic dicarboxylate ligand', Journal of Coordination Chemistry, 64: 2, 244 — 255, First published on: 13 December 2010 (iFirst)

To link to this Article: DOI: 10.1080/00958972.2010.540651

URL: http://dx.doi.org/10.1080/00958972.2010.540651

Journal of Coordination Chemistry
Vol. 64, No. 2, 20 January 2011, 244–255

Metal–organic supramolecular architectures derived from a new zwitterionic dicarboxylate ligand

XIU-MEI ZHANG, XIU-BING LI and EN-QING GAO*

Shanghai Key Laboratory of Green Chemistry and Chemical Processes, Department of Chemistry, East China Normal University, Shanghai 200062, P.R. China

(*Received 28 July 2010; in final form 19 October 2010*)

A series of new coordination compounds with 1-carboxymethylpyridinium-4-benzoate (L) and transition metal ions have been synthesized. They are formulated as $[M(L)_2(H_2O)_4]\cdot 4H_2O$ M=Mn (**1**) and Co (**2**), $\{[M(L)_2]\cdot xH_2O\}_n$ M=Mn, $x=1$ (**3**); M=Co, $x=2$ (**4**), and M=Cu, $x=3$ (**5**). In **1** and **2**, the zwitterionic dicarboxylate ligand is monodentate through only one carboxylate to generate mononuclear molecules. The molecules are assembled through O–H $\cdots$ O interactions to give 3-D pillared layer-like architectures, in which interesting 1-D tape-like hydrogen bonding motifs are connected into 2-D layers *via* carboxylate-mediated hydrogen bonds. In **3–5**, the organic ligands serve as bridges with one carboxylate monodentate and the other chelating, and the metal ions are linked by double bridges to give 1-D polymeric chains, which are zigzag (**3**) or stair-like (**4** and **5**) due to the *cis* or *trans* coordination geometry around metal ions. The chains are further stabilized and associated into 3-D architectures through intra- and interchain hydrogen bonding and/or π–π stacking interactions.

Keywords: Hydrogen bonds; Zwitterionic ligand; Manganese(II); Cobalt(II); Copper(II)

1. Introduction

Metal–organic architectures assembled through combined coordinative and non-covalent interactions have gained widespread interest in supramolecular chemistry and coordination chemistry due to their structural diversity and potential applications [1–18]. The metal–ligand coordination may lead to discrete or extended coordination motifs, the structures primarily dependent on electronic and geometric properties of the organic ligands and metal ions. Other interactions, such as hydrogen bonding, may reinforce the coordination motifs or assemble discrete or low-dimensional motifs into higher-dimensional architectures [9–18]. Solvent molecules may also influence the final supramolecular assemblies by participating in metal coordination and hydrogen bonding. The final architecture can be regarded as the interplay between coordination and hydrogen bonding forces [18–24]. The metal–ligand coordination can direct hydrogen bonding patterns by gathering and disposing the hydrogen bonding sites around metal ions in a specific fashion, and the hydrogen bonding may impose perturbations on the coordination mode or the ligand conformation. Carboxylates can

---

*Corresponding author. Email: eqgao@chem.ecnu.edu.cn

Journal of Coordination Chemistry
ISSN 0095-8972 print/ISSN 1029-0389 online © 2011 Taylor & Francis
DOI: 10.1080/00958972.2010.540651

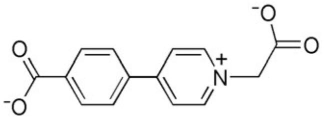

Scheme 1. Chemical structure of L.

bind metal ions in various modes and form various hydrogen bonding motifs and hence have been widely employed to construct metal–organic materials. Currently, the most frequently used are di- and multi-carboxylate ligands with neutral spacers between carboxylates [25–33]. The coordination chemistry of zwitterionic carboxylate ligands, which contain positive groups such as pyridinium, has been studied for decades but to less lower extent [34–38]. The previously used zwitterionic ligands are usually neutral in the coordinated form (the negative carboxylate is charge compensated by the positive group). Lying between ordinary and neutral ligands, zwitterionic ligands that contain more carboxylates than positive groups and hence have reduced negative charge have received little attention in coordination chemistry and crystal engineering [39–41]. The charge on the carboxylate will certainly influence the coordination and supramolecular structures. In continuation of our recent work [39, 40], here we report five coordination compounds derived from different transition metal ions and a new zwitterionic dicarboxylate (L, scheme 1), which has not been explored in coordination chemistry before. The compounds are $[M(L)_2(H_2O)_4]\cdot 4H_2O$ M=Mn (**1**) and Co (**2**), $\{[M(L)_2]\cdot xH_2O\}_n$ M=Mn, $x=1$ (**3**); M=Co, $x=2$ (**4**), and M=Cu, $x=3$ (**5**). Compounds **1** and **2** are mononuclear, while **3–5** are 1-D coordination polymers. In all these compounds, hydrogen bonding and π–π stacking sustain the coordination structure and associate the coordination motifs into 3-D architectures.

2. Experimental

2.1. *Physical measurements*

Elemental analyses were determined on an Elementar Vario ELIII analyzer. FT-IR spectra were recorded from 500 to 4000 cm^{-1} using KBr pellets on a Nicolet NEXUS 670 spectrophotometer.

2.2. *Synthesis*

The reagents were obtained from commercial sources and used without purification. The new ligand was prepared according to a procedure for similar compounds [42].

2.2.1. $[Mn(L)_2(H_2O)_4]\cdot 4H_2O$ (1). A mixture of $MnCl_2\cdot 4H_2O$ (0.010 g, 0.050 mmol) and L (0.024 g, 0.10 mmol) in H_2O/CH_3OH (3/2 mL) was stirred at room temperature and then filtered. Slow evaporation of the solution at room temperature yielded white crystals of **1** within 2 days. Yield: 60%. Anal. Calcd (%) for $C_{28}H_{36}MnN_2O_{16}$: C, 47.27; H, 5.10; and N, 3.94. Found (%): C, 47.59; H, 4.88; and N, 4.07.

IR (KBr, cm^{-1}): 3372(w), 3073(m), 1647(s), 1565(m), 1536(m), 1474(w), 1374(s), 1322(w), 1245(w), 1203(m), 919(w), 785(w), 755(w), 728(w), 690(w), and 648(w).

2.2.2. $[Co(L)_2(H_2O)_4]\cdot 4H_2O$ (2). A procedure similar to that for **1** was followed to prepare **2** using $CoCl_2\cdot 6H_2O$ instead of $MnCl_2\cdot 4H_2O$. Red crystals were collected within 3 days. Yield: 55%. Anal. Calcd (%) for $C_{28}H_{36}CoN_2O_{16}$: C, 47.00; H, 5.07; and N, 3.92. Found (%): C, 47.13; H, 5.31; and N, 3.89. IR (KBr, cm^{-1}): 3308(w), 3039(m), 1647(s), 1566(s), 1532(m), 1478(w), 1375(m), 1327(w), 1260(m), 1203(w), 920(w), 782(m), 754(w), 686(m), and 591(w).

2.2.3. $\{[Mn(L)_2]\cdot H_2O\}_n$ (3). A mixture of $MnCl_2\cdot 4H_2O$ (0.010 g, 0.050 mmol) and L (0.024 g, 0.10 mmol) was dissolved in H_2O (3 mL) and CH_3OH (2 mL) in a Teflon-lined stainless steel vessel (25 mL), heated at 70°C for 3 days under autogenous pressure, and then cooled to room temperature. Red block crystals were harvested. Yield: 54% based on Mn. Anal. Calcd (%) for $C_{28}H_{22}MnN_2O_9$: C, 57.45; H, 3.79; and N, 4.79. Found (%): C, 57.24; H, 4.15; and N, 4.50. IR (KBr, cm^{-1}): 3368(w), 3261(m), 3074(m), 1641(s), 1567(m), 1535(m), 1378(s), 1320(w), 1203(m), 1012(w), 973(w), 922(w), 843(w), 822(w), 783(m), 727(w), 691(w), and 641(w).

2.2.4. $\{[Co(L)_2]\cdot 2H_2O\}_n$ (4). A procedure similar to that for **3** was followed to prepare **4** using $CoCl_2\cdot 6H_2O$ instead of $MnCl_2\cdot 4H_2O$. Red crystals were obtained in 50% yield. Anal. Calcd (%) for $C_{28}H_{24}CoN_2O_{10}$: C, 55.36; H, 3.98; and N, 4.16. Found (%): C, 55.27; H, 4.37; and N, 4.35. IR (KBr, cm^{-1}): 3418(br), 3076(m), 2921(m), 2852(w), 1642(s), 1568(m), 1535(m), 1378(s), 1323(w), 1203(m), 1012(w), 974(w), 826(w), 784(w), 755(m), 727(w), 692(w), and 642(w).

2.2.5. $\{[Cu(L)_2]\cdot 3H_2O\}_n$ (5). A procedure similar to that for **1** was followed to prepare **5** using $CuCl_2\cdot 2H_2O$ instead of $MnCl_2\cdot 4H_2O$. Blue crystals were obtained in 55% yield. Anal. Calcd (%) for $C_{28}H_{26}CuN_2O_{11}$: C, 53.38; H, 4.16; and N, 4.45. Found (%): C, 52.89; H, 4.33; and N, 4.40. IR (KBr, cm^{-1}): 3487(m), 3375(m), 3063(m), 2921(m), 1642(s), 1600(w), 1560(w), 1538(w), 1375(s), 1305(w), 1199(m), 924(w), 848(m), 788(w), 760(w), 729(w), 698(w), and 648(w).

2.3. *Crystal data collection and refinement*

Diffraction data were collected at 293 K on a Bruker Apex II CCD area detector equipped with graphite-monochromated Mo-Kα radiation ($\lambda = 0.71073$ Å). Empirical absorption corrections were applied using the SADABS program [43]. The structures were solved by direct methods and refined by full-matrix least-squares on F^2, with all non-hydrogen atoms refined with anisotropic thermal parameters [44]. All hydrogens attached to carbon were placed in calculated positions and refined using the riding model, and the water hydrogens in **1**, **2**, **4**, and **5** were located from difference maps. The hydrogens of lattice water in **3**, which is disordered with an occupancy of 0.5, were not located. All calculations were carried out with the SHELXTL crystallographic software. A summary of the crystallographic data, data collection, and refinement parameters for **1**–**5** are given in table 1.

3. Results and discussion

3.1. *Description of the crystal structures*

3.1.1. Compounds 1 and 2. Single crystal X-ray analyses revealed that **1** and **2** are isomorphic with 3-D hydrogen bond networks. On going from Mn to Co, the M–O distances and cell dimensions exhibit systematic decrease, consistent with the variation in metal ionic radii. Otherwise, the two structures show only very minor difference, so only the structure of **1** is described here in detail. The relevant parameters are given in table 2. The structure consists of mononuclear $[Mn(L)_2(H_2O)_4]$ and lattice water. The molecule has a site symmetry of $2/m$, in which the Mn(II) assumes the *trans*-octahedral coordination geometry completed by two equivalent carboxyl oxygens (O1, O1C) at axial positions and four equivalent waters (O4, O4A, O4B, O4C) in the equatorial plane (figure 1). The dicarboxylate ligand, with the methylenecarboxylate moiety in the crystallographic *m*-plane and the 4-(4-pyridyl)benzenecarboxylate moiety bisected by the plane, is monodentate, using only the methylenecarboxylate for coordination, although the other carboxylate is also deprotonated.

The carboxylate groups and water molecules, which are gathered around the metal ion in the specific geometry, provide a rich store of hydrogen bonding sites for intermolecular interactions. The relevant hydrogen bonding parameters are given in table 3. As shown in figure 1, the molecules are arranged in a complementary way so that the uncoordinated carboxylate from one molecule can be doubly hydrogen bonded to a pair of coordinated waters from another molecule, forming a hydrogen bonding ring with graph-set symbol $R_2^2(8)$ (figure 1) [45]. Consequently, each molecule is linked to two identical molecules *via* four pairs of hydrogen bonds to generate a chain along the *c*-direction. The chain consists of centrosymmetric rectangular bimetallic rings that share the metal corners. The two phenylene groups in the bimetallacycle are parallel and overlapped with interplanar and center-to-center distances of 3.566(4) Å and 3.730(1) Å, respectively, suggesting that the hydrogen-bonded chain is reinforced by π–π interactions.

The remaining donor and acceptor sites are involved in complicated hydrogen bonding with lattice water, which assemble the chains into 3-D architectures. An interesting 1-D hydrogen-bonded tape-like motif is formed along the *c*-direction. To form the main line of the tape, neighboring metal ions are doubly linked by pairwise O–H $\cdots$ O $\cdots$ H–O hydrogen bonding bridges, in which the central bifurcate acceptors are from lattice water (O5) and the donors are aqua ligands from different metal ions. There are three independent hydrogen bonding rings in the tape. The largest one, $R_4^2(12)$, is the central motif consisting of two metal ions (Mn $\cdots$ Mn = 7.122(1) Å), four-coordinated water molecules as donors, and two lattice water molecules (O5) as bifurcate acceptors. The second is the above-mentioned $R_2^2(8)$ motif consisting of a Mn(II), two water ligands and a carboxylate as acceptors; the third consists of water ligands as double donors, two lattice waters (O5 and O6) as donor and acceptor, and a carboxylate oxygen as bifurcate acceptor [$R_4^3(8)$]. To complete the four-coordination,

Table 1. Crystal data and structure refinement for **1**–**5**.

Compound	**1**	**2**	**3**	**4**	**5**
Empirical formula	$C_{28}H_{36}MnN_2O_{16}$	$C_{28}H_{36}CoN_2O_{16}$	$C_{28}H_{22}MnN_2O_9$	$C_{28}H_{24}CoN_2O_{10}$	$C_{28}H_{26}CuN_2O_{11}$
Formula weight	711.53	715.52	585.42	607.42	630.06
Crystal system	Monoclinic	Monoclinic	Monoclinic	Triclinic	Triclinic
Space group	$C2/m$	$C2/m$	$C2/c$	$P\bar{1}$	$P\bar{1}$
Unit cell dimensions (Å, °)					
a	14.7384(18)	14.5705(6)	14.3571(5)	7.6319(15)	7.5678(8)
b	7.1217(9)	7.0987(3)	8.3297(3)	8.4352(17)	8.1550(8)
c	15.1516(19)	15.0946(7)	20.4974(8)	10.971(2)	11.4237(11)
α	90	90	90	84.41(3)	83.3430(10)
β	90.995(2)	91.2200(10)	91.6990(10)	76.83(3)	79.3440(10)
γ	90	90	90	68.48(3)	70.3140(10)
Volume (Å^3), Z	1590.1(3), 2	1560.90(12), 2	2450.21(16), 4	639.7(2), 1	651.27(11), 1
Calculated density (Mg m^{-3})	1.486	1.522	1.538	1.577	1.606
Absorption coefficient (mm^{-1})	0.494	0.630	0.596	0.736	0.908
$F(000)$	742	746	1164	313	325
Crystal size (mm^3)	0.30 × 0.20 × 0.10	0.30 × 0.20 × 0.10	0.30 × 0.20 × 0.08	0.30 × 0.10 × 0.08	0.30 × 0.20 × 0.10
θ range for data collection (°)	2.69–27.50	1.35–28.45	1.99–28.25	1.91–25.00	2.66–25.00
Limiting indices	$-16 \le h \le 19$; $-8 \le k \le 9$; $-17 \le l \le 19$	$-18 \le h \le 19$; $-9 \le k \le 9$; $-19 \le l \le 20$	$-19 \le h \le 19$; $-11 \le k \le 10$; $27 \le l \le 25$	$-8 \le h \le 9$; $-4 \le k \le 10$; $-13 \le l \le 13$	$-8 \le h \le 8$; $-9 \le k \le 9$; $-13 \le l \le 6$
Reflections collected	4986	10,672	15,876	2624	4077
Independent reflection	1956 [R(int) = 0.0210]	2105 [R(int) = 0.0231]	3013 [R(int) = 0.0299]	2190 [R(int) = 0.0482]	2250 [R(int) = 0.0113]
Data/restraints/parameters	1956/0/142	2105/0/142	3013/0/186	2190/0/187	2250/3/205
Goodness-of-fit on F^2	1.000	1.063	1.040	1.093	1.055
Final R indices [$I > 2\sigma(I)$]	$R_1 = 0.0374$, $wR_2 = 0.0880$	$R_1 = 0.0304$, $wR_2 = 0.0950$	$R_1 = 0.0417$, $wR_2 = 0.1141$	$R_1 = 0.0788$, $wR_2 = 0.2188$	$R_1 = 0.0319$, $wR_2 = 0.0885$
R indices (all data)	$R_1 = 0.0446$, $wR_2 = 0.0931$	$R_1 = 0.0342$, $wR_2 = 0.1064$	$R_1 = 0.0713$, $wR_2 = 0.1342$	$R_1 = 0.0813$, $wR_2 = 0.2237$	$R_1 = 0.0340$, $wR_2 = 0.0903$
Largest difference peak and hole (e Å^{-3})	0.195 and −0.275	0.410 and −0.296	0.280 and −0.422	1.586 and −1.822	0.517 and −0.253

Table 2. Selected bond lengths (Å) and angles (°) for **1** and **2**.

	1 (M=Mn)	**2** (M=Co)
M1–O1	2.171(2)	2.085(1)
M1–O4	2.176(1)	2.096(1)
O1A–M1–O1	180.0	180.00(2)
O1–M1–O4A	92.11(5)	91.88(4)
O1–M1–O4	87.89(5)	88.12(4)
O4–M1–O4A	180.00(5)	180.00(4)
O4–M1–O4B	89.22(7)	90.83(6)
O4–M1–O4C	90.78(7)	89.17(6)

Symmetry transformations used to generate equivalent atoms: A: $-x+1$, $-y+1$, $-z+1$; B: x, $-y+1$, z; C: $-x+1$, y, $-z+1$.

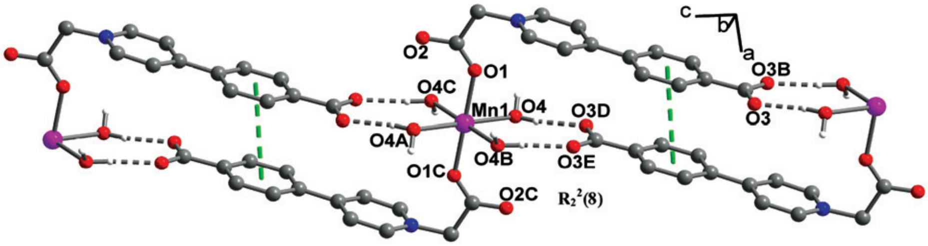

Figure 1. The 1-D coordination chain in which mononuclear molecules are linked by hydrogen bonds in **1**.

Table 3. Hydrogen bond lengths (Å) and angles (°) for **1** and **2**.

D	A[transformation]	*d*(D–H)	*d*(H···A)	*d*(D···)	∠(DHA)
O4	O3[$-x+1$, $-y+1$, $-z$]	0.84(2)	1.87(2)	2.706(2)	172(2)
		0.84(2)	1.88(2)	2.713(2)	161(3)
O4	O5	0.86(3)	1.87(3)	2.732 (2)	172(2)
		0.77(2)	1.98(2)	2.741(2)	168(2)
O5	O2[$-x+1/2$, $-y+1/2$, $-z+1$]	0.91(4)	1.76(4)	2.673(3)	178(3)
		0.79(4)	1.90(4)	2.686(2)	173(4)
O5	O6	0.82(4)	2.01(4)	2.799(3)	161(4)
		0.85(4)	1.97(4)	2.803(3)	167(3)
O6	O3[$-x+1$, $-y+1$, $-z$]	0.85(3)	2.03(3)	2.853(2)	162(3)
		0.75(3)	2.12(3)	2.840(2)	161(3)

D, donor; A, acceptor. For each entry, the first and second data are for **1** and **2**, respectively.

the O5 from one tape is hydrogen bonded to the uncoordinated O2 of the monodentate carboxylate from another tape. Consequently, the tapes are associated in a self-complementary way to produce a hydrogen-bonded 2-D network along the *ab*-plane (figure 2b). The whole 3-D structure may be regarded as a pillared multilayer architecture, where the ligands serve as pillars between the hydrogen-bonded layers (figure 2c).

3.1.2. Compound 3. The structure of **3** consists of 1-D coordination chains. The chain structure is shown in figure 3(a), with selected bond distances and angles given

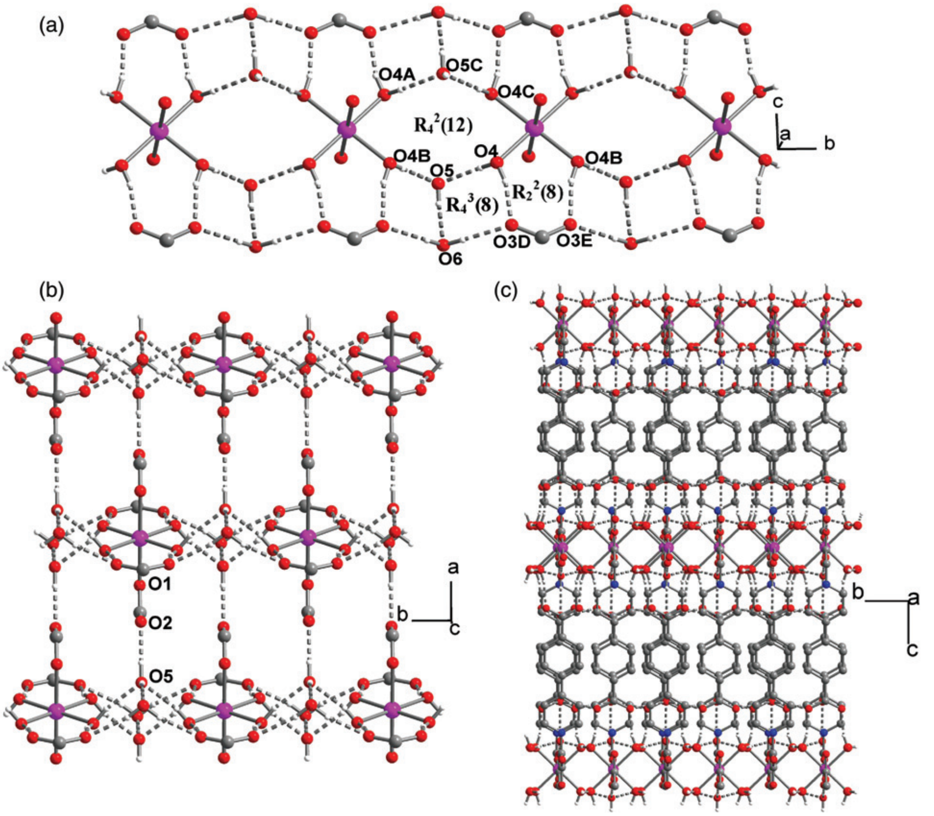

Figure 2. (a) A hydrogen-bonded tape in **1**. (b) The 2-D hydrogen bonding layer structure. (c) The 3-D pillared-layer-like architecture of **1**.

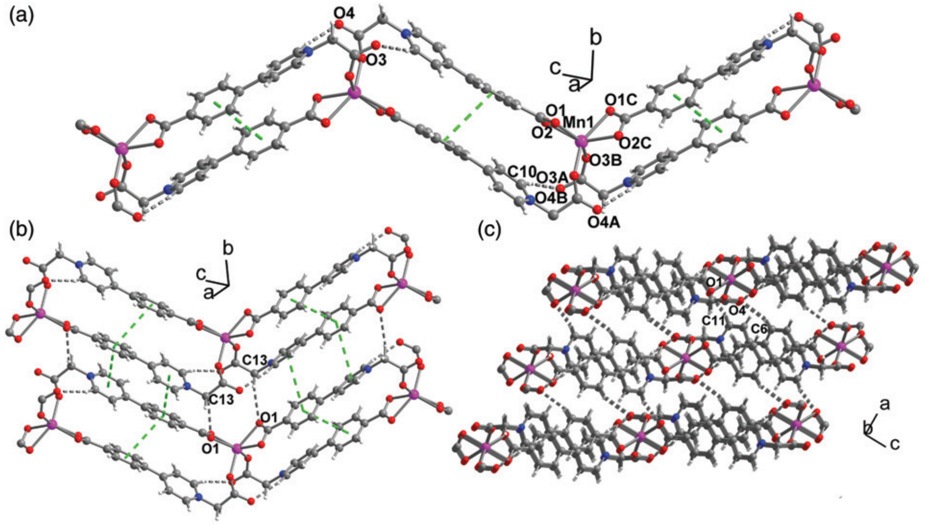

Figure 3. (a) The 1-D coordination chain in **3**. (b) A view of the π–π stacking and hydrogen bonds between the chains. (c) The 3-D packing in **3**.

Table 4. Selected bond lengths (Å) and angles (°) for **3**.

Mn1–O3A	2.086(2)	Mn1–O1	2.311(2)
Mn1–O2	2.211(2)		
O3A–Mn1–O3B	95.43(11)	O3B–Mn1–O1	149.45(7)
O3A–Mn1–O2	110.67(7)	O2–Mn1–O1	57.10(8)
O3B–Mn1–O2	94.29(8)	O1–Mn1–O1C	107.21(12)
O2–Mn1–O2C	142.93(12)	O2C–Mn1–O1	99.55(7)
O3A–Mn1–O1	86.40(8)		

Symmetry transformations used to generate equivalent atoms: A: $-x+1/2$, $-y+1/2$, $-z$; B: $x-1/2$, $-y+1/2$, $z-1/2$; C: $-x$, y, $-z-1/2$.

in table 4. The unique Mn(II) resides on a twofold axis and exhibits a highly distorted octahedral coordination geometry occupied by four oxygens (O1, O2, O1C, and O2C) from two equivalent chelating carboxylate groups and other two oxygens (O3A, O3B) at *cis* positions from two equivalent monodentate carboxylates. The zwitterionic ligand uses its two carboxylates to bind two Mn(II) ions in chelating and monodentate modes, respectively. The adjacent Mn(II) centers are connected by a pair of zwitterionic ligands to form a centrosymmetric and rectangular bimetallic ring, and adjacent rings share the metal center to form a 1-D zigzag-like chain along the (1 0 1) direction. The coordination chain is further reinforced by π–π interaction between the centrosymmetry-related phenylene groups in the bimetallacycle (the interplanar and center-to-center distances are 3.600(3) Å and 3.841(1) Å, respectively) and the weak C–H $\cdots$ O hydrogen bonding between a pyridyl C–H group to the uncoordinated carboxylate oxygen [C10 $\cdots$ O4 3.211(3) Å]. There are also interchain C–H $\cdots$ O hydrogen bonding and π–π stacking interactions. Offset π–π interaction occurs between phenylene and pyridyl rings from different chains with only edge-to-edge overlap [46], the interplanar and center-to-center distances being 3.756(3) Å and 4.092(1) Å, respectively. Hydrogen bonding involves the methylene C13–H from one chain and the coordinated O1 from another chain [C13 $\cdots$ O1 3.495(1) Å]. These interchain interactions help to align the zigzag chains in corner-in-corner fashion, generating a 2-D layer along the $(1\,0\,\bar{1})$ plane (figure 3b). The layers are further packed into the 3-D architecture through two independent sets of weak hydrogen bonds [C6 $\cdots$ O4 3.456(3) Å and C11 $\cdots$ O1 3.067(4) Å] (figure 3c). The parameters for the weak hydrogen bonds are listed in the "Supplementary material" (supplementary table S1).

3.1.3. Compounds 4 and 5.

Compounds **4** and **5** are pseudo-isomorphous, since they crystallize in the same space group, exhibit similar crystal structures, but have different numbers of lattice waters. The relevant parameters are given in table 5.

The coordination mode of the zwitterionic ligand in **4** and **5** is similar to that in **3**, and the metal center is also six-coordinate by four carboxylates, two chelating, and two monodentate. However, as shown in figure 4(a), the metal ion resides at a crystallographic inversion center, and the equivalent carboxylates are at opposite positions around the metal ion, generating a *trans*-octahedral configuration in contrast to the *cis* one in **3**. The metal ions in **4** and **5** are also doubly linked by the organic ligands to give 1-D chains (along the $(0\,1\,\bar{1})$ direction) consisting of centrosymmetric and rectangular bimetallacycles. However, as a result of the change of the coordination

Table 5. Selected bond lengths (Å) and angles (°) for **4** and **5**.

	4 (M=Co)	**5** (M=Cu)
M1–O3A	2.042(3)	1.954(2)
M1–O1	2.135(3)	1.977(2)
M1–O2	2.163(3)	2.532(2)
O3A–M1–O3B	180.0	180.0
O3A–M1–O1	94.36(1)	94.69(6)
O3B–M1–O1	85.64(1)	85.31(6)
O1–M1–O1C	180.0	180.0
O3A–M1–O2	95.30(1)	97.25(6)
O3B—M1–O2	84.70(1)	82.75(6)
O1–M1–O2	61.32(1)	57.15(6)
O1C–M1–O2	118.68(1)	122.85(6)
O2–M1–O2C	180.0	180.0

Symmetry transformations used to generate equivalent atoms: A: x, $y-1$, $z+1$; B: $-x+1$, $-y+1$, $-z+1$; C: $-x+1$, $-y$, $-z+2$.

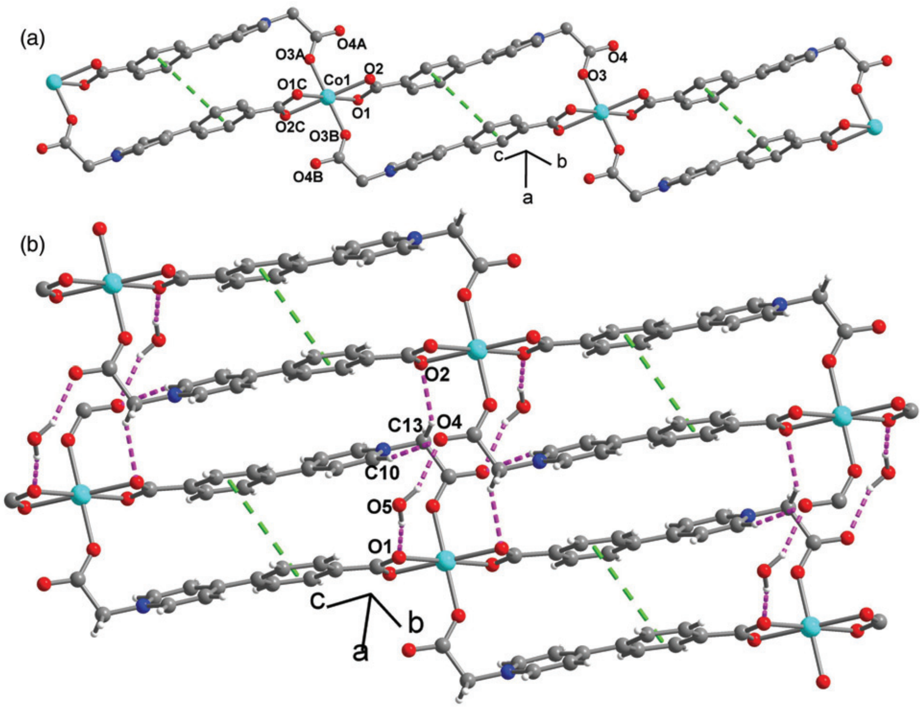

Figure 4. (a) The 1-D coordination chain in **4**. (b) The 2-D layer in **4** assembled through hydrogen bonding interactions.

configuration from *trans* to *cis*, the chain in **4** and **5** has a stair-like, instead of zigzag-like, shape, with all metal ions collinear along the chain. There is also intrachain π–π interaction between the phenylene groups in **4** and **5** (the interplanar and center-to-center distances being respectively 3.625(6) Å and 4.086(5) Å for **4**, and 3.529(2) Å and 3.972(2) Å for **5**), but the intrachain C–H···O hydrogen bonding observed in **3** is impossible in **4** and **5**. As shown in figure 4(a), the chains in **4** and **5** are aligned in an

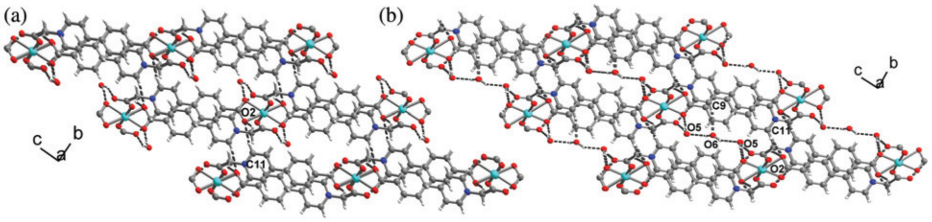

Figure 5. The 3-D packing of the layers in **4** (a) and **5** (b).

edge-to-edge fashion to give a thin layer parallel to the (0 1 1) plane, and the neighboring chains along the layer are associated *via* weak C–H···O hydrogen bonds involving the methylene groups and coordinated oxygens (O2) and O–H···O hydrogen bonds mediated by uncoordinated water. The water (O5) donates its hydrogens to an uncoordinated oxygen (O4) from one chain and a coordinated oxygen (O1) from another chain. There are also weak C–H···O hydrogen bonds between neighboring layers (figure 5); the hydrogen bonding parameters for **4** and **5** are given in table S2.

Despite the above structural similarity of **4** and **5**, the two compounds are different in other aspects. In **4**, the chelating carboxylate has two similar Co–O distances (2.163(3) Å and 2.135(3) Å), but the distance for the monodentate carboxylate is shorter (2.042(2) Å); so the *trans*-octahedral geometry around Co(II) is somewhat compressed along the axis defined by the two monodentate carboxylates. By contrast, the chelating carboxylate in **5** is highly asymmetric, with significantly different Cu–O distances, 2.532(2) Å and 1.977(2) Å. The shorter one is similar to that for the monodentate carboxylate (1.954(2) Å); so the geometry around Cu(II) is significantly elongated along one of the two axes defined by the two chelating carboxylates. The difference reflects the larger Jahn–Teller effects of the Cu(II)-$t_{2g}^6e_g^3$ configuration than the Co(II)-$t_{2g}^5e_g^2$ configuration. Besides the distance distortion, the geometry also exhibits very large angular distortion due to the small bite angles of the chelating carboxylates (57.15(6)° and 61.32(1)°), and the angle distortion in **5** is even larger than that in **4**, which is related to the highly asymmetric chelating mode in **5**.

As mentioned above, both structures have a lattice water (O5) per asymmetric unit that forms hydrogen bonds with carboxylates from different chains in the layer along the (0 1 1) plane. Compound **5** has an additional lattice molecule (O6) per metal ion, which is disordered over two equivalent positions sharing the hydrogens. However, the presence of this molecule does not impose significant influence on the packing structure. It is simply inserted between hydrogen bonded to two O5 waters associated with different layers (figure 5b). In **4**, the distance between the corresponding O5 atoms is too close to allow insertion of the additional water. The subtle difference between **4** and **5** is presumed to be due to the interplay and compromise between the coordination requirements of the metal ions and various supramolecular interactions, but it is impossible to propose an explanation on the detailed mechanism.

4. Conclusions

We have described a series of metal–organic architectures derived from divalent metal ions and a new zwitterionic ligand with overall −1 charge, which contains two carboxylates and a pyridinium-based spacer. The compositions and structures are quite different from those for compounds with −2 charged dicarboxylates based on neutral spacers or the neutral ones based on *bis*(pyridinium) spacers. Compounds **1** and **2** contain mononuclear molecules assembled into 3-D hydrogen-bonded architectures through O–H $\cdots$ O interactions involving carboxylate and water. In **3**–**5**, the organic ligands serve as double bridges between metal ions to generate 1-D coordination chains, which are zigzag (**3**) or stair-like (**4** and **5**) due to the *cis* or *trans* coordination geometry around metal ions. The coordination chains, reinforced by intrachain π–π stacking in **3**–**5** and also by intrachain weak C–H $\cdots$ O interactions in **3**, are associated through interchain hydrogen bonding interactions (and also π–π interactions in **3**) to give 3-D supramolecular architectures.

Supplementary material

Crystallographic data as .cif files for the structures reported in this article have been deposited with the Cambridge Crystallographic Data Center. CCDC numbers are 784769–784773. Copies of the data can be obtained free of charge from CCDC, 12 Union Road, Cambridge CB2 1EZ, UK.

Acknowledgments

We thank National Natural Science Foundation of China (NSFC) (20771038) and Shanghai Leading Academic Discipline Project (B409) for providing financial support.

References

[1] B.H. Ye, M.L. Tong, X.M. Chen. *Coord. Chem. Rev.*, **249**, 545 (2005).
[2] S.L. James. *Chem. Soc. Rev.*, **32**, 276 (2003).
[3] O.M. Yaghi, M. O'Keeffe, N.W. Ockwig, H.K. Chae, M. Eddaoudi, J. Kim. *Nature*, **423**, 705 (2003).
[4] S. Kitagawa, R. Kitaura, S. Noro. *Angew. Chem. Int. Ed.*, **43**, 2334 (2004).
[5] B.J. Holliday, C.A. Mirkin. *Angew. Chem. Int. Ed.*, **40**, 2022 (2001).
[6] H. Oshio, Y. Saito, T. Ito. *Angew. Chem. Int. Ed. Engl.*, **36**, 2673 (1997).
[7] C. Janiak. *Dalton Trans.*, 2781 (2003).
[8] M.S. Ray, A. Ghosh, R. Bhattacharya, G. Mukhopadhyay, M.G.B. Drew, J. Ribas. *Dalton Trans.*, 252 (2004).
[9] A.D. Burrows, C.-W. Chan, M.M. Chowdhry, J.E. McGrady, D.M.P. Mingos. *Chem. Soc. Rev.*, **24**, 329 (1995).
[10] M.D. Stephenson, M.J. Hardie. *CrystEngComm*, **9**, 496 (2007).
[11] N. Lui, Y.Q. Wang, E.Q. Gao, Z.X. Chen, L.H. Weng. *CrystEngComm*, **10**, 915 (2008).
[12] Y. Ma, A.L. Cheng, C.Y. Tian, H. Tian, E.Q. Gao. *J. Mol. Struct.*, **935**, 129 (2009).
[13] G.W. Yang, Q.Y. Li, Y. Zhou, G.Q. Gu, Y.S. Ma, R.X. Yuan. *Inorg. Chim. Acta*, **362**, 1234 (2009).
[14] H. Tian, Q.X. Jia, Y.Q. Wang, Y. Ma, E.Q. Gao. *J. Mol. Struct.*, **933**, 8 (2009).
[15] K. Uemura, K. Saito, S. Kitagawa, H. Kita. *J. Am. Chem. Soc.*, **128**, 16122 (2006).
[16] M.J. Calhorda. *Chem. Commun.*, 801 (2000).
[17] L.J. Zhou, Y.Y. Wang, C.H. Zhou, C.J. Wang, Q.Z. Shi, S.M. Peng. *Cryst. Growth Des.*, **7**, 300 (2007).
[18] A.M. Beatty. *Coord. Chem. Rev.*, **246**, 131 (2003).
[19] J.R. Li, Y. Tao, Q. Yu, X.H. Bu. *Cryst. Growth Des.*, **6**, 2493 (2006).

[20] T.L. Hu, W.P. Du, B.W. Hu, J.R. Li, X.H. Bu, R. Cao. *CrystEngComm*, **10**, 1037 (2008).
[21] R.Q. Zou, C.S. Liu, Z. Huang, T.L. Hu, X.H. Bu. *Cryst. Growth Des.*, **6**, 99 (2006).
[22] M.P. Lightfoot, F.S. Mair, R.G. Pritchard, J.E. Warren. *Chem. Commun.*, 1945 (1999).
[23] C.M. Jin, Z.F. Chen, C.Y. Chen, J.H. Dong. *J. Coord. Chem.*, **62**, 390 (2009).
[24] C.M. Jin, Z. Zhu, Z.F. Chen, Y.J. Hu, X.G. Meng. *Cryst. Growth Des.*, **10**, 2054 (2010).
[25] A.L. Cheng, Y. Ma, J.Y. Zhang, E.Q. Gao. *Dalton Trans.*, 1993 (2008).
[26] Q. Yue, X.B. Qian, L. Yan, E.Q. Gao. *Inorg. Chem. Commun.*, **11**, 1067 (2008).
[27] J.S. Costa, P. Gamez, C.A. Black, O. Roubeau, S.J. Teat, J. Reedijk. *Eur. J. Inorg. Chem.*, 1551 (2008).
[28] B. Moulton, M.J. Zaworotko. *Chem. Rev.*, **101**, 1629 (2001).
[29] Y. Yang, Y.F. Feng, N. Liang, B.L. Li, Y. Zhang. *J. Coord. Chem.*, **62**, 3819 (2009).
[30] F. Luo, M.B. Luo, X.L. Tong. *J. Coord. Chem.*, **63**, 1147 (2010).
[31] D. Feng, S.X. Liu, P. Sun, F.J. Ma, W. Zhang. *J. Coord. Chem.*, **63**, 1737 (2010).
[32] L.Q. Yang, G. Zhan, S.C. Jia, Q. Shi, X.H. Li. *J. Coord. Chem.*, **63**, 2056 (2010).
[33] H.Y. He, D.Q. Yuan, H.Q. Ma, D.F. Sun, G.Q. Zhang, H.C. Zhou. *Inorg. Chem.*, **49**, 7605 (2010).
[34] B.J.V. Quagliano, S. Kida, J. Fujita. *J. Am. Chem. Soc.*, **84**, 724 (1962).
[35] M.Y. Chow, Z.Y. Zhou, T.C.W. Mak. *Inorg.Chem.*, **31**, 4900 (1992).
[36] X.M. Chen, T.C.W. Mak. *Inorg. Chem.*, **33**, 2444 (1994).
[37] Y. Ikegami, T. Muramatsu, K. Hanaya, S. Onodera, N. Nakayama, E.M. Kosowerld. *J. Am. Chem. Soc.*, **109**, 2876 (1987).
[38] X.M. Chen, T.C.W. Mak. *J. Mol. Struct.*, **249**, 135 (1991).
[39] X.M. Zhang, Y.Q. Wang, E.Q. Gao. *Eur. J. Inorg. Chem.*, 1249 (2010).
[40] Y.Q. Wang, K. Wang, Q. Sun, H. Tian, E.Q. Gao, Y. Song. *Dalton Trans.*, 9854 (2009).
[41] C.X. Ming, T.C.W. Mak. *Aust. J. Chem.*, **44**, 1783 (1991).
[42] S.J. Loeb, J. Tiburcio, S.J. Vella, J.A. Wisner. *Org. Biomol. Chem.*, **4**, 667 (2006).
[43] G.M. Sheldrick. *Program for Empirical Absorption Correction of Area Detector Data*, University of Göttingen, Göttingen, Germany (1996).
[44] G.M. Sheldrick. *SHELXTL Version 5.1*, Bruker Analytical X-ray Instruments Inc., Madison, Wisconsin, USA (1998).
[45] M.C. Etter. *Acc. Chem. Res.*, **23**, 120 (1990).
[46] C. Janiak. *J. Chem. Soc., Dalton Trans.*, 3885 (2000).